Acta Mechanica 101, 1 – 13 (1993)

ACTA MECHANICA

Stability of axial Poiseuille-Couette flow between concentric cylinders

Ph. Gittler, Vienna, Austria

(Received July 8, 1992)

Summary. The linear stability of axial parallel Poiseuille-Couette flow in an annulus between concentric circular cylinders is considered. Using a long-wave version of the axisymmetric Orr-Sommerfeld equation the stability chart of this flow in the velocity ratio-radius ratio plane is derived. It is shown that pure sliding Couette flow can become unstable if the radius ratio is below a specific threshold value. Finally, applying the results to other flow geometries, it is shown that the boundary layer along a slender cylinder can become unstable in a confined region downstream the leading edge only.

1 Introduction

The hydrodynamic linear stability of viscous flows has received considerable attention in view of its importance in the mechanism of the natural transition from laminar to turbulent flows. This paper is devoted to the investigation of linear stability of the axial flow of an incompressible Newtonian fluid in the annulus between concentric circular cylinders. The stability characteristics of annular Poiseuille flow were first analyzed by Mott and Joseph [8] and this flow was found to be unstable, unlike the Hagen-Poiseuille flow in a circular pipe. The case of annular sliding Couette motion was investigated recently by Preziosi and Rosso [12] and they did not find any indication of linear instability.

The present investigation examines the stability properties of combined axial Poiseuille-Couette flow in a cylindrical annulus. One does not know a priori whether a superposition of Couette flow on Poiseuille flow will cause the flow to be more or less stable. This problem was investigated in the case of plane flow by Potter [11] and later by Cowley and Smith [1]. Their methods are applied to the cylindrical flow geometry in Section 2 of this paper and the solutions of the governing equations are presented in Sections 3 and 4. One important result, the linear instability of annular sliding Couette flow (in contrast to the findings of Preziosi and Rosso [12]) is given in Section 5. Finally, the application of the results to annular Poiseuille flow and to the boundary layer flow along a semi-infinite cylinder is discussed in Section 6.

2 Problem formulation

We consider the incompressible, axial flow in the annulus between two concentric cylinders with radii $\tilde{R}_1$ and $\tilde{R}_2$ ($\tilde{R}_1 < \tilde{R}_2$), see Fig. 1. Throughout this study, dimensional quantities are denoted by superscript $\tilde{}$. $(\tilde{u}, \tilde{v}, \tilde{w})^T$ denotes the velocity vector in the cylindrical coordinate system $(\tilde{r}, \phi, \tilde{z})^T$. The motion of the fluid is generated by a fixed axial pressure gradient (Poiseuille flow,

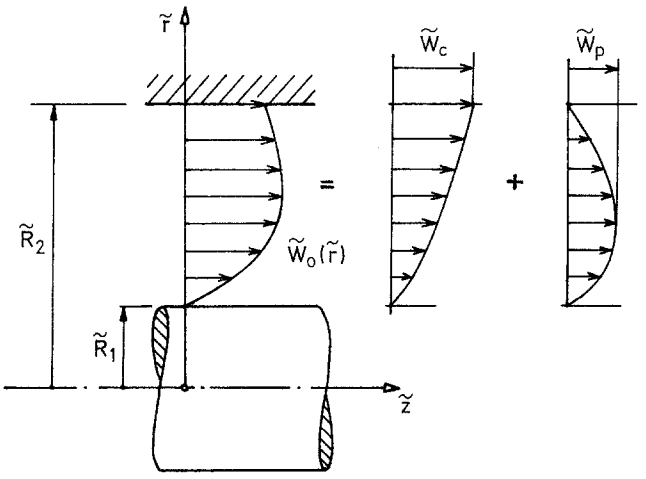

Fig. 1. Poiseuille-Couette flow in a cylindrical annulus

maximum velocity $\tilde{W}_p$) and/or by the sliding velocity of the outer cylinder $\tilde{W}_c$ (Couette flow). The analysis in this paper will be restricted to axisymmetric motions and disturbances, i.e. $\partial/\partial\phi \equiv 0$.

Three nondimensional parameters enter the problem:

$$\text{the radius ratio } \eta = \tilde{R}_1/\tilde{R}_2,$$

$$\text{the velocity ratio } K_c = \tilde{W}_c/\tilde{W}_p \tag{1}$$

$$\text{and the Reynolds number } \mathrm{Re} = \tilde{W}_{ref}\tilde{R}_1/\tilde{\nu}.$$

η varies within the range $0 \leqq \eta \leqq 1$. The limit $\eta \to 0$ characterizes the single inner cylinder in unbounded flow while $\eta \to 1$ corresponds to the case of plane motion. $\tilde{\nu}$ denotes the kinematic viscosity. For the present the reference velocity $\tilde{W}_{ref}$ is taken to be $\tilde{W}_p$ (later on in the case of pure Couette flow we will take $\tilde{W}_{ref} = \tilde{W}_c$). We scale the lengths with $\tilde{R}_1$, the velocities with $\tilde{W}_{ref}$, the pressure with $\tilde{\varrho}\tilde{W}_{ref}^2$ and the time with $\tilde{R}_1/\tilde{W}_{ref}$ to obtain nondimensional quantities. The governing Navier-Stokes equations can be integrated to yield the velocity distribution of the unperturbed basic flow

$$W_0(r) = \frac{1 - \eta^2 r^2 + \gamma(\ln r + \ln \eta)}{1 - \gamma(1 - \ln \gamma/2)/2} - K_c \frac{\ln r}{\ln \eta}, \tag{2}$$

with $\gamma = (\eta^2 - 1)/\ln \eta$.

As usual, the stream function for the small disturbances is harmonic in z and t, with the wave number α and the complex phase speed $c = c_r + ic_i$:

$$\Psi(r, z, t) = \Phi(r) \exp\left[i\alpha(z - ct)\right]. \tag{3}$$

For the non-harmonic component $\Phi(r)$ we get after insertion of (3) into the Navier-Stokes equations and linearization the axisymmetric Orr-Sommerfeld equation

$$\Phi^{iv} - \frac{2}{r}\Phi''' + \left[\frac{3}{r^2} - 2\alpha^2 - i\alpha\,\mathrm{Re}\,(W_0 - c)\right]\left(\Phi'' - \frac{1}{r}\Phi'\right)$$
$$+ \left\{\alpha^4 + i\alpha\,\mathrm{Re}\left[W_0'' - \frac{W_0'}{r} + \alpha^2(W_0 - c)\right]\right\}\Phi = 0. \tag{4.1}$$

Imposing the boundary conditions

$$\Phi(1) = \Phi'(1) = \Phi(1/\eta) = \Phi'(1/\eta) = 0 \tag{4.2}$$

we thus obtain the eigen-value problem describing the linear stability characteristics of axisparallel Poiseuille-Couette flows between concentric cylinders. The eigen-value problem requires that $c_i = 0$ if no growth or decay of the disturbance is allowed. The minimum Reynolds number of the neutral-stability curve representing the above relationship is the critical Reynolds number Re_{cr}.

Annular Poiseuille flow ($\tilde{W}_c = 0$) was studied first by Mott and Joseph [8] for axisymmetric disturbances. Asymmetric disturbances were taken into account later by Mahadevan and Lilley [7] and Dzygadlo and Chlebny [3]. All these investigations show that Re_{cr} increases without bound as the radius ratio $\eta \to 0$, starting from the plane Poiseuille flow limit $\eta = 1$ (see Section 5, Fig. 9). The authors argue that the velocity distribution assumes the Hagen Poiseuille form as the inner cylinder vanishes ($\eta \to 0$) which explains the unrestricted stabilisation of the flow in this limit. This point will be discussed again later in Section 5.

Preziosi and Rosso [12] investigated pure annular sliding Couette flow ($\tilde{W}_p = 0$) and state the result: "... the flow always turns out to be linearly stable". As will be shown later this is only true for a limited range of the radius ratio η.

In this study we will consider the stability of axisparallel, annular Poiseuille Couette flow. In the case of plane motions ($\eta = 1$) Poiseuille flow has a finite critical Reynolds number while Couette flow always behaves linearly stable. Potter [11] was the first to investigate the question how the superposition of these two flows influences the overall stability properties. Starting from plane Poiseuille flow, $K_c = 0$, his results show an increase of Re_{cr} for increasing values of K_c. As K_c approaches a cut-off value, $K_c^* \approx 0.70$, Re_{cr} tends to infinity and the neutral curve disappears. Therefore plane Poiseuille-Couette flow is always stable to infinitesimal disturbances if the Couette component exceeds $\sim 70\%$ of the maximum Poiseuille velocity. As can be imagined the calculation of K_c^* as a function of η using this method would be a very cumbersome procedure.

In [1] Cowley and Smith introduced an asymptotic method to compute "exactly" the cut-off value K_c^* for plane Poiseuille-Couette flow. This method makes use of the fact that the asymptotic behaviour of the neutral curves for $K_c = 0(1)$ is given by $\alpha = 0(\mathrm{Re}^{-1})$ for large Re in contrast to pure Poiseuille flow where $\alpha = 0(\mathrm{Re}^{-1/7})$ and $0(\mathrm{Re}^{-1/11})$ on the lower and upper branch, respectively. Using the parameter $\lambda = 1/(\alpha\,\mathrm{Re})$ which is constant in the limit $\mathrm{Re} \to \infty$, $\alpha \to 0$, Cowley and Smith formulated a somewhat simplified "long-wave" eigen-value problem whose solution is sketched in Fig. 2. The two values λ_l and λ_u corresponding to each value K_c, for $K_c < K_c^*$, define the asymptotes of lower and upper branch of the neutral curve. For $K_c^* = 0.704$ the two branches coalesce and the neutral curve disappears. If $K_c \geqq K_c^*$ the flow is always linearly stable.

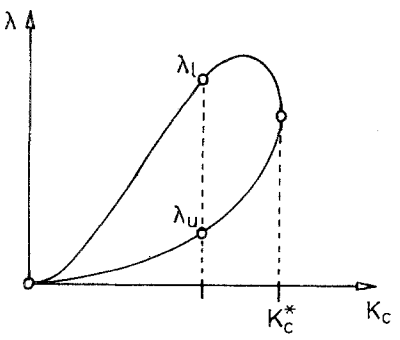

Fig. 2. Qualitative sketch of the long-wave eigenvalue relation according to Eq. (5)

Let us now apply this method to annular Poiseuille-Couette flow. Equation (4) in the limit $\mathrm{Re} \to \infty$, with $\lambda = 1/(\alpha\,\mathrm{Re}) = \text{const}$, takes the form

$$\Phi^{iv} - \frac{2}{r}\Phi''' + \left[\frac{3}{r^2} - \frac{i}{\lambda}(W_0 - c)\right]\left(\Phi'' - \frac{1}{r}\Phi'\right) + \frac{i}{\lambda}\left(W_0'' - \frac{W_0'}{r}\right)\Phi = 0$$

$$\Phi(1) = \Phi'(1) = \Phi(1/\eta) = \Phi'(1/\eta) = 0 \tag{5}$$

corresponding to a long wave version of the cylindrical Orr-Sommerfeld equation.

3 Method of solution

The eigen-value problem (5) was solved numerically by means of the Compound Matrix Method which was applied to hydrodynamic stability problems for the first time by Ng and Reid [9]. A short description of this method can be found for instance in Drazin and Reid [2]. By means of the Compound Matrix Method the two point boundary value problem is simply changed to an initial value problem which can be solved using a standard integrator. This yields the eigenvalue relation in form of a complex-valued function $F(\lambda, c_r; \eta, K_c)$ and the zeros of F determine the eigenvalues in dependence on the parameters.

The Compound Matrix Method has the advantage of giving very accurate results which was the main reason for adopting it in this investigation, since the eigen-value problems (4) and (5) develop complex numerical properties for small values of η. As a minor drawback the method requires very good initial guesses for the eigenvalues. Starting with a radius ratio of $\eta = 0.8$ and $\lambda = 2.2 \cdot 10^{-6}$ it was impossible to get converged eigenvalues by means of the usual Newton-Raphson iteration procedure.

To clarify the reason for this failure the eigenvalue relation F was calculated at a large number of values of c_r and k_c (gridpoints). Then the contours of Re $(F) = 0$ and Im $(F) = 0$ were plotted by means of interpolation between the gridpoints, Fig. 3a. This contour plot — showing two intersection points, i.e. two eigenvalues where Re (F) = Im $(F) = 0$ — reveals the handicap of the Compound Matrix Method: the eigenvalue relation has a strong oscillatory behaviour indicated by the large number of nearly straight lines in almost constant distance. Therefore, in a modified

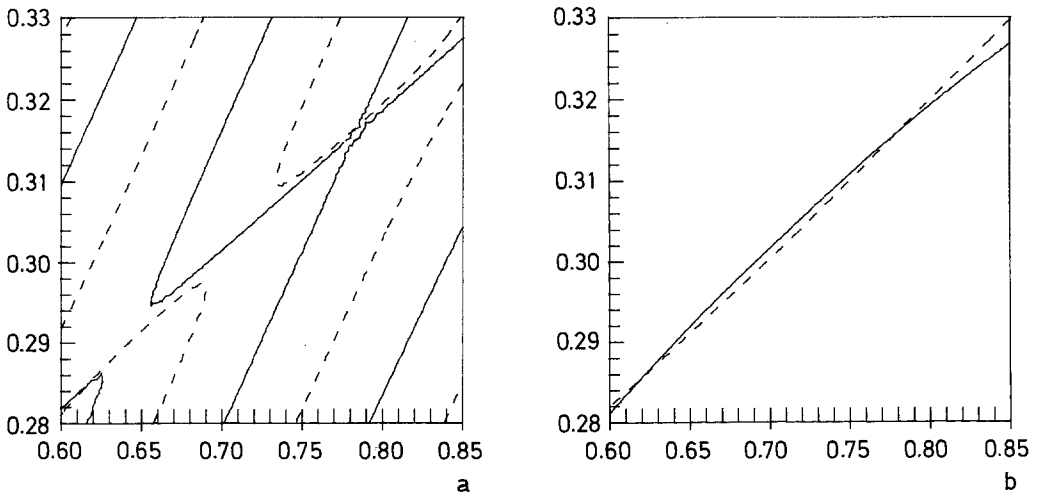

Fig. 3. Contour plot of the eigenvalue relation F for $\eta = 0.8$, $\lambda = 2.2 \cdot 10^{-6}$; —— Re$(F) = 0$, - - - - Im$(F) = 0$. **a** Original Compound Matrix Method; **b** modified version

numerical scheme the complex-valued function F is smoothed by multiplication with an experimental term $\bar{F} = F \exp[i(\gamma c_r + \varkappa K_c)]$; herein the complex coefficients γ and $\varkappa$ are computed automatically by the program. The improvement can immediately be seen in Fig. 3 b. One can imagine, the Newton-Raphson procedure now needs much less accurate initial guesses to get a converged eigenvalue. Together with a similar modification which helps to suppress oscillations occuring during the integrations of the Compound Matrix equations it was possible to speed up the computations by a factor between 5 and 10.

4 The long wave eigen-value problem

Figure 4 shows the main results of the numerical computations of the long wave problem: the stability chart for axisparallel annular Poiseuille-Couette flow in the $K_p - \eta$ plane. ($K_p = 1/K_c$ is more suitable for a clear and simple graphical presentation of the results.) For $\eta = 1$, representing the plane flow situation, we can apply Potter's result: the flow is linearly stable if the relative Poiseuille component $K_p = W_p/W_c$ is less than a cut-off value $K^*_{pu} = 1.42 = 1/0.704$. The same limit applies for negative Poiseuille components, $K^*_{pl} = -1.42$, since the velocity profiles are identical for positive and negative values K_p and $-K_p$ in the plane case ($\eta = 1$). In the cylindrical annulus ($\eta < 1$) we get different velocity distributions and, therefore, we have to compute separately the second, lower stability boundary $K^*_{pl}(\eta)$ in addition to the upper one $K^*_{pu}(\eta)$. Inside the shaded regions ($K_p > K^*_{pu}$ or $K_p < K^*_{pl}$) the flow always exhibits a neutral stability curve with a finite critical Reynolds number Re_{cr}.

Each point of the stability boundaries K^*_{pu} or K^*_{pl} corresponds to the apex of the upper or lower marginal curve defined by the long wave eigen-value problem (5) for a given value of η. To compute these boundaries for decreasing values of η an automatic search algorithm with 2nd

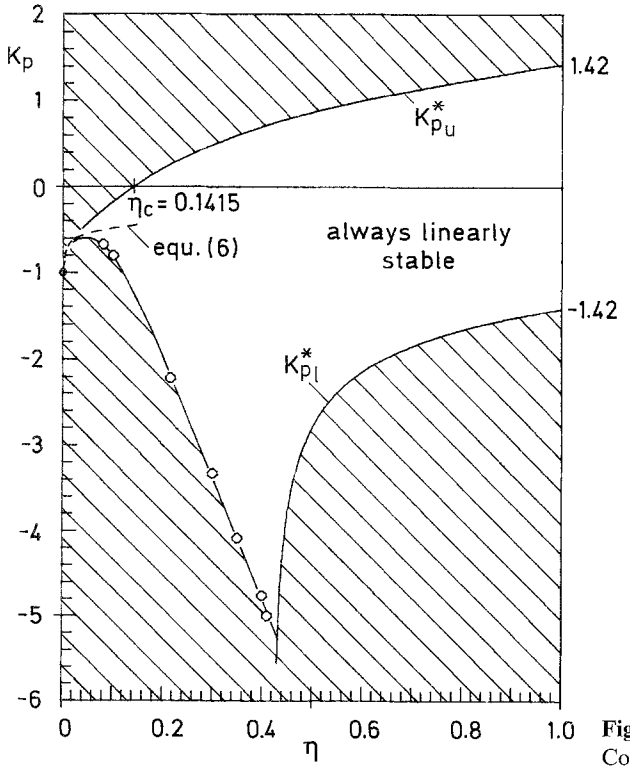

Fig. 4. Stability chart for annular Poiseuille-Couette flow

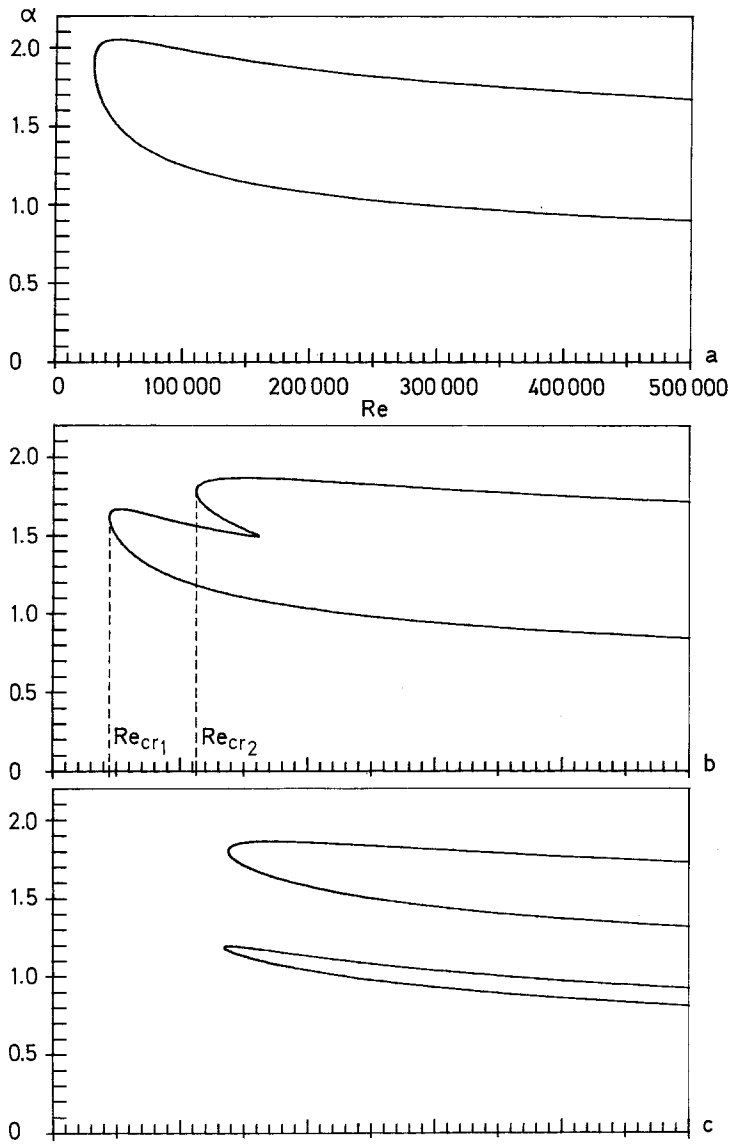

Fig. 5. Marginal curves for $\eta = 0.5$ and **(a)** $K_c = 0$, **(b)** $K_c = -0.05$, and **(c)** $K_c = -0.07$

order tracking using small $\Delta\eta$ steps was implemented. The results for K_{pl}^* ended with a vertical slope near $\eta = 0.428$ and no solution of the eigen-value problem (5) in continuing the lower stability boundary for $\eta < 0.428$ could be found. To close the stability chart in this region the full Orr-Sommerfeld problem, Eq. (4), has to be investigated. Characteristic results for $\eta = 0.5$ are presented in Fig. 5. Figure 5a shows the neutral-stability curve for pure annular Poiseuille flow ($K_c = 0$) in the wave number – Reynolds number plane. Adding a small negative Couette component of $K_c = -0.04$ changes the neutral curve significantly, as can be seen from Fig. 5b. A second apex is formed and a further decrease of K_c results in a splitting of the curve, Fig. 5c, with two corresponding critical Reynolds numbers Re_{cr1} and Re_{cr2}.

These critical Reynolds numbers are depicted in Fig. 6a as functions of the velocity ratio K_c for $\eta = 0.5$. The stability of the flow for $-0.121 < K_c < -0.070$ is determined by the second neutral curve, since $\mathrm{Re}_{cr2} < \mathrm{Re}_{cr1}$ in this interval. For $K_c < -0.121$ the change from stable to unstable behaviour is given again by Re_{cr1} which tends to infinity as K_c approaches the cut-off

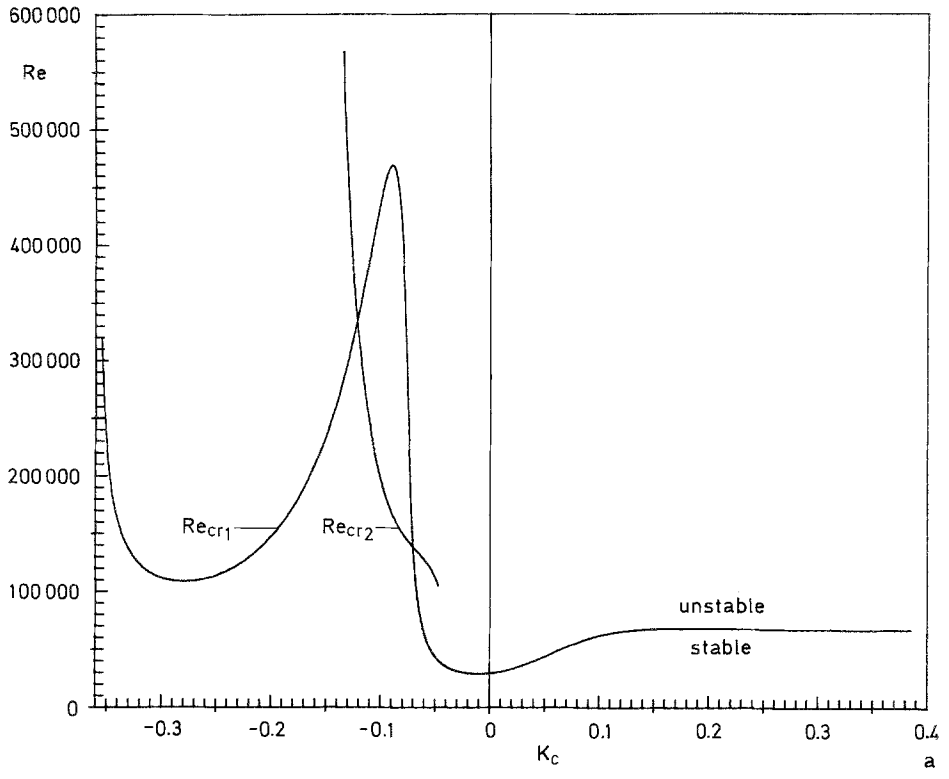

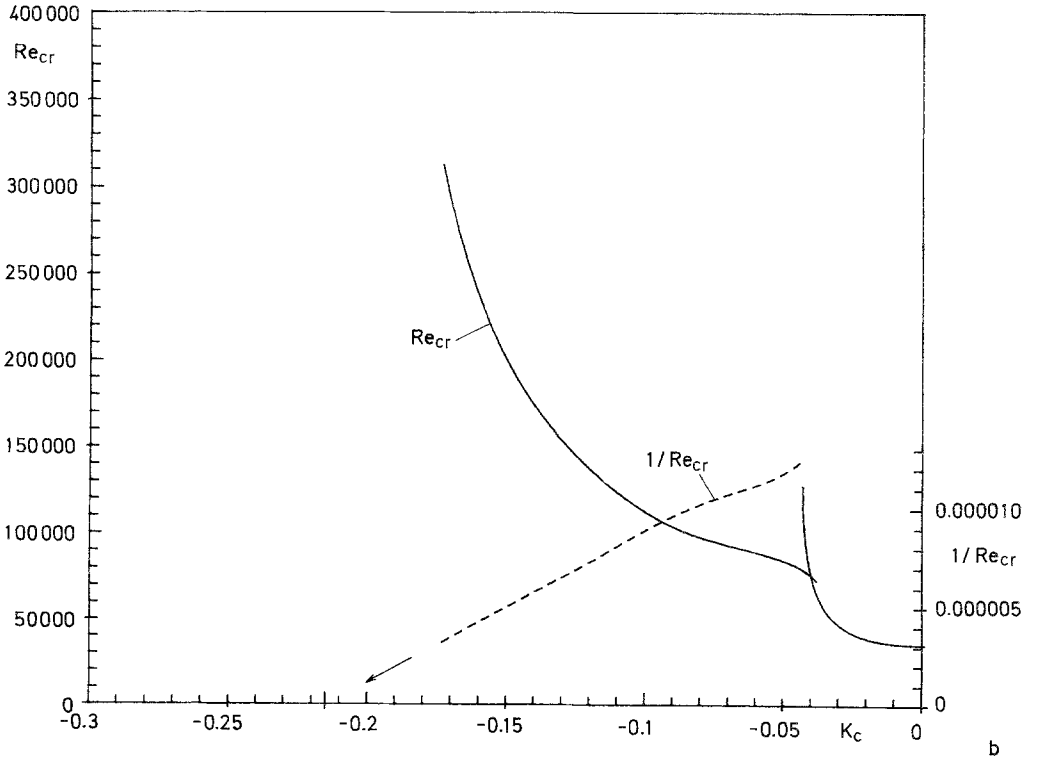

Fig. 6. Critical Reynolds numbers for **(a)** $\eta = 0.5$ and **(b)** $\eta = 0.4$

value $K_{cl}^* = 1/K_{pl}^* = -0.3584$ in agreement with the long wave results, eigen-value problem (5), Fig. 4. An analogous plot of $\mathrm{Re}_{cr}(K_c)$ for $\eta = 0.4$ is shown in Fig. 6b. For decreasing values of K_c, after the change from Re_{cr1} to Re_{cr2} and the vanishing of the first neutral curve, Re_{cr2} continues to be the determining critical Reynolds number of the flow. Since this second neutral curve does not exhibit the asymptotic behaviour $\alpha \sim 1/\mathrm{Re}$ for $\mathrm{Re} \to \infty$, on both the upper and the lower branch, the long wave eigen-value problem (5) cannot be applied (and yields no solution). Therefore, the cut-off value K_{cl}^* has to be determined directly from the Orr-Sommerfeld results.

As can be seen from Fig. 6b it is useful to plot the $1/\mathrm{R}_{cr} - K_c$ relationship which turned out to be nearly a straight line in the limit $\mathrm{Re}_{cr} \to \infty$. Extrapolation of the numerical results with acceptable accuracy then yields $K_{cl}^*(\eta = 0.4) = -0.215$. Finally the value $K_{pl}^*(\eta = 0.4) = -1/0.215 = -4.65$ is indicated by a small circle in Fig. 4. Using six additional values – obtained by the same cumbersome procedure – it was possible to close the stability chart, Fig. 4.

A useful asymptote for the relationship $K_p(\eta)$ holding in the limit $\eta \to 0$ can be obtained by the following simple argument. Since the instability of the flow for $\eta \to 0$ is triggered by the shear stress near the surface of the inner cylinder a velocity distribution $W_0(r)$ with $dW_0/dr(r = 1) = 0$ must always yield stable behaviour. For vanishing wall shear stress we thus get

$$K_{p0}(\eta) = \left[1 + \frac{\gamma}{2}\left(\ln\frac{\gamma}{2} - 1\right)\right] \Big/ [\eta^2(1 - 2\ln\eta) - 1] \tag{6}$$

with $\gamma(\eta)$ defined in Eq. (2). This result, shown as a broken line in Fig. 4, is in complete agreement with the numerical calculations in the limit $\eta \to 0$ (with $K_{p0}(\eta \to 0) = -1$).

5 Annular sliding Couette flow

The most striking feature of the stability chart is the fact that the upper stability boundary K_{pu}^* crosses the η-axis ($K_p = 0$). This indicates that pure annular sliding Couette flow can become unstable for $\eta < \eta_c = 0.1415$ (in contrast to the statement of Preziosi and Rosso [12] who considered larger values of η only). We now turn to the full Orr-Sommerfeld problem (4) to investigate the stability characteristics of this axial Couette flow. The marginal curves for the radius ratio $\eta = 0.1$ are depicted in Fig. 7 and they exhibit the usual shape, characteristic for a shear induced instability. The critical Reynolds number, based on the sliding velocity of the outer cylinder ($\tilde{W}_{ref} = \tilde{W}_c$), is found to be $\mathrm{Re}_{cr}(\eta = 0.1) = 8.026 \cdot 10^5$. From Fig. 7b we find the critical wave speed $c_{cr} = 0.0379$; together with the velocity distribution $W_0(r) = -\ln r/\ln\eta$ for $1 \leqq r \leqq 1/\eta$ this yields the location of the critical layer $r_{cr}(\eta = 0.1) = 1.091$.

Figure 8 shows the influence of η on the critical values Re_{cr}, c_{cr} and α_{cr} for axial Couette flow. In complete agreement with the long wave results instability sets in for η less than $\eta_c = 0.1415$. With decreasing η-values, Re_{cr} decreases until it reaches its minimum value at $\eta = 0.08$, before it starts to increase again tending to infinity for $\eta \to 0$. This behaviour can be explained in the following way: Initially, the flow becomes more unstable as the gap width increases. For sufficiently small values of η however, another counteracting effect comes into operation. Since the reference velocity is the sliding velocity of the outer cylinder which moves outwards as η decreases, the shear stress which evokes the instability in the critical layer $r = r_{cr}$ near the inner surface decreases, resulting in an increase of Re_{cr}. This suggests a new velocity-scaling: The velocity distribution

$$W_0(r) = \tilde{W}_0/\tilde{W}_{ref} = \ln r \tag{7.1}$$

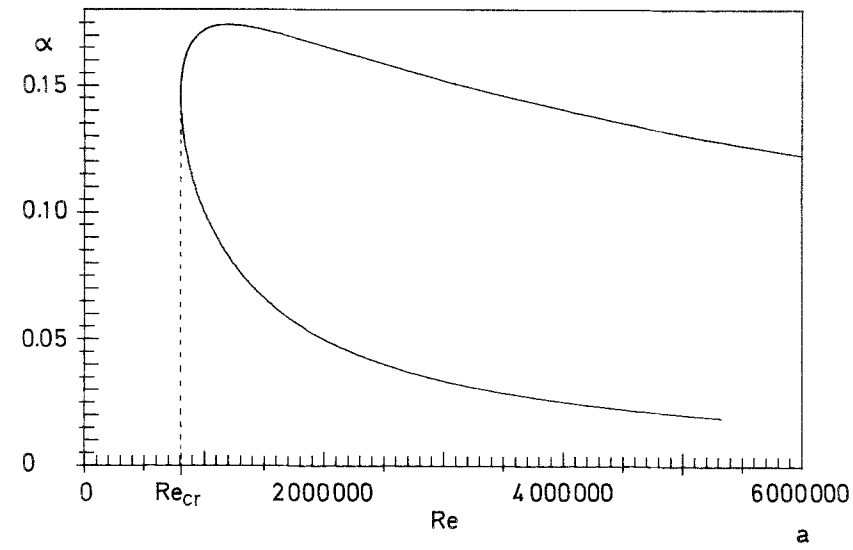

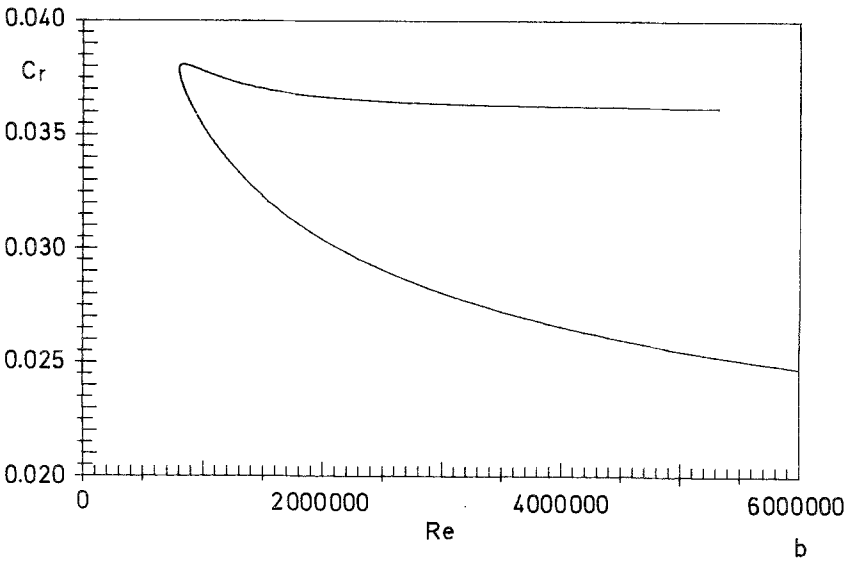

Fig. 7. Marginal curves for annular sliding Couette flow for $\eta = 0.1$ **(a)** wave number α, **(b)** phase speed c_r

with the reference velocity expressed by the wall shear stress $\tilde{\tau}_W$ and the radius $\tilde{R}_1$ of the inner cylinder

$$\tilde{W}_{ref} = \tilde{\tau}_W \tilde{R}_1 / \tilde{\mu} \tag{7.2}$$

remains unchanged as the outer boundary $\tilde{R}_2$ goes to infinity. Therefore we have to replace the Reynolds number Re by $\mathrm{Re}/(-\ln \eta)$ and the phase speed c by $c(-\ln \eta)$ whereas the wave number α remains unchanged. As can be seen from these rescaled results (broken lines in Fig. 8) the influence of the outer cylinder on the stability properties vanishes if $\eta \leqq 0.05$ (that means $\tilde{R}_2 \geqq 20\, \tilde{R}_1$) since all three critical values become approximately constant. For smaller values of η the numerical solution of the eigenvalue problem becomes extremely difficult. However, results could be obtained down to $\eta = 0.01$.

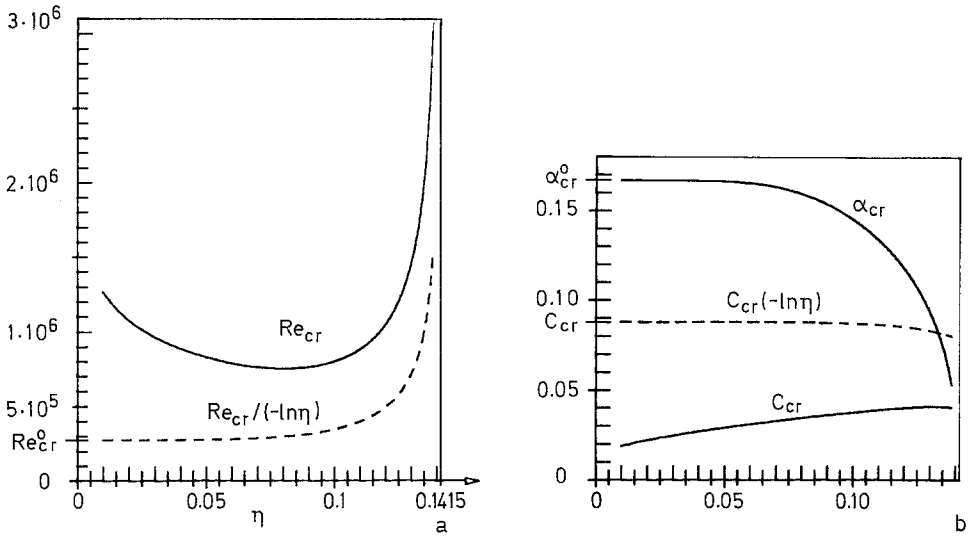

Fig. 8. Critical values for annular sliding Couette flow: **(a)** Re_{cr}, **(b)** c_{cr} and α_{cr}

Carrying out the limit $\eta \to 0$ ($\tilde{R}_2 \to \infty$) we have thus obtained the stability characteristics of an unbounded fluid flow along a single cylinder $\tilde{R}_1$ with the logarithmic velocity profile (7):

$$
\begin{aligned}
&Re^0_{cr} = (\tilde{\varrho}\tilde{\tau}_W \tilde{R}_1{}^2)/\tilde{\mu}^2 = 2.7530 \cdot 10^5, \\
&\alpha^0_{cr} = 0.16681, \\
&c^0_{cr} = 0.087709.
\end{aligned}
\tag{8}
$$

6 Applications and discussion of the results

Let us first apply this result to annular Poiseuille flow in the limit $\eta \to 0$ [Eq. (2) with $K_c = 0$]. Figure 9 shows the influence of the radius ratio η on the critical Reynolds number, as already discussed in Section 2. The numerical solution given by the solid line is in complete agreement with the results of Strumolo [15]. The Reynolds number in Fig. 9 is based on the average velocity $\langle \tilde{W} \rangle$

$$
\langle \mathrm{Re} \rangle = \frac{(\tilde{R}_2 - \tilde{R}_1)\,\langle \tilde{W} \rangle}{2\tilde{\nu}}, \tag{9}
$$

$$
\langle \tilde{W} \rangle = \frac{1 + \eta^2 - \gamma}{2 + \gamma(\ln \gamma/2 - 1)}\,\tilde{W}_p \quad \text{with} \quad \gamma = (\eta^2 - 1)/\ln \eta.
$$

Accordingly, the critical value in the case of plane motion is given by $\langle \mathrm{Re} \rangle_{cr} = (2/3).5772.2 = 3848.1$ (cf. Orszag [10]). In the limit $\eta \to 0$ the ln-term in the velocity distribution becomes more and more dominant in the vicinity of the inner cylinder and therefore, Eq. (8) can be applied to yield:

$$
\langle \mathrm{Re} \rangle_{cr}\,(\eta \to 0) = 2.753 \cdot 10^5 \frac{(1 - \eta)\,(1 + \eta^2 - \gamma)}{2\eta(2\gamma - 4\eta^2)}. \tag{10}
$$

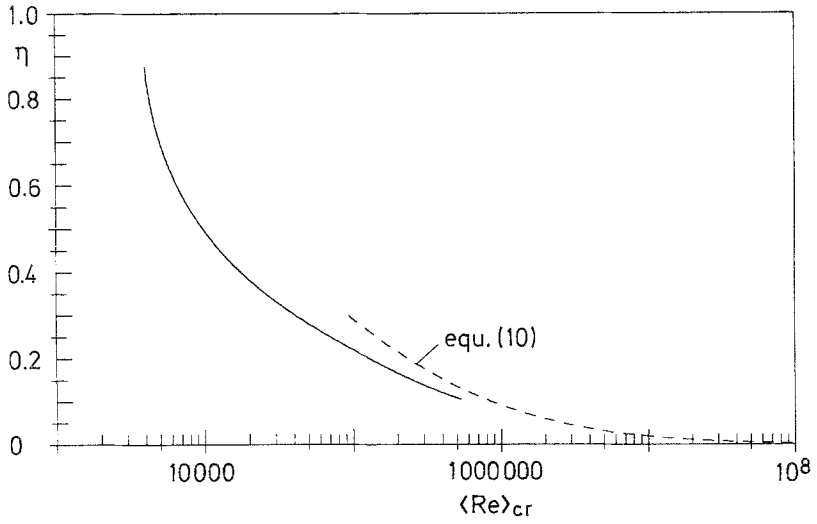

Fig. 9. Critical Reynolds number for annular Poiseuille flow

This asymptotic relationship, shown in Fig. 9, is in very good correspondence with the numerical results. As a consequence, the assumption that the flow approaches the linearly stable Hagen-Poiseuille flow in a pipe seems to be incorrect. Rather there is always an instability near the surface of the inner cylinder whose critical values become constant in the limit $\eta \to 0$ if the proper scaling – based on the wall shear stress $\tilde{\tau}_W$ and the radius $\tilde{R}_1$ of the inner cylinder – is used.

Another problem to which the result (8) can be successfully applied is the axisymmetric laminar boundary layer flow along a semi-infinite cylinder of constant radius $\tilde{R}$. The constant free-stream velocity is denoted by $\tilde{W}_\infty$. As shown by Glauert and Lighthill [4] and Stewartson [14] the velocity distribution inside the boundary layer near the surface is given to leading order by the logarithmic profile (7). The flow is characterized by two Reynolds numbers, defined with the radius $\tilde{R}$ and the axial coordinate $\tilde{z}$, respectively

$$\mathrm{Re}_R = \tilde{W}_\infty \tilde{R}/\tilde{\nu} \quad \text{and} \quad \mathrm{Re}_z = \tilde{W}_\infty \tilde{z}/\tilde{\nu}. \tag{11}$$

According to Eq. (8) instability sets in for $\tilde{\tau}_W \tilde{\varrho} \tilde{R}^2/\mu^2 \geqq 2.7530 \cdot 10^5$. Using Glauert and Lighthill's result, valid far downstream, this condition can be expressed as

$$\mathrm{Re}_{R_{cr}} = 2.7530 \cdot 10^5 \ln(\xi/2) \quad \text{for} \quad \xi \to \infty \tag{12.1}$$

with ξ – a suitably scaled axial coordinate – given by

$$\xi = 4\sqrt{\mathrm{Re}_z}/\mathrm{Re}_R. \tag{12.2}$$

Figure 10 represents the stability chart for the boundary layer flow along a cylinder in the $\mathrm{Re}_R - \xi$ plane. For given free stream velocity $\tilde{W}_\infty$, radius $\tilde{R}$ and viscosity $\tilde{\nu}$, i.e. $\mathrm{Re}_R = \text{const}$, we are interested to find the values of ξ for which linear instability of the flow sets in. Since the wall shear stress $\tilde{\tau}_W$ decreases for $\xi \to \infty$ the region of unstable flow is located upstream of the dashed line, defined by the asymptotic relationship (12.1), shown at the right hand side in the upper part of Fig. 10. Therefore, using linear theory and applying parallel flow assumption, the boundary layer stabilizes again when passing the stability boundary (12.1) downstream along the cylinder.

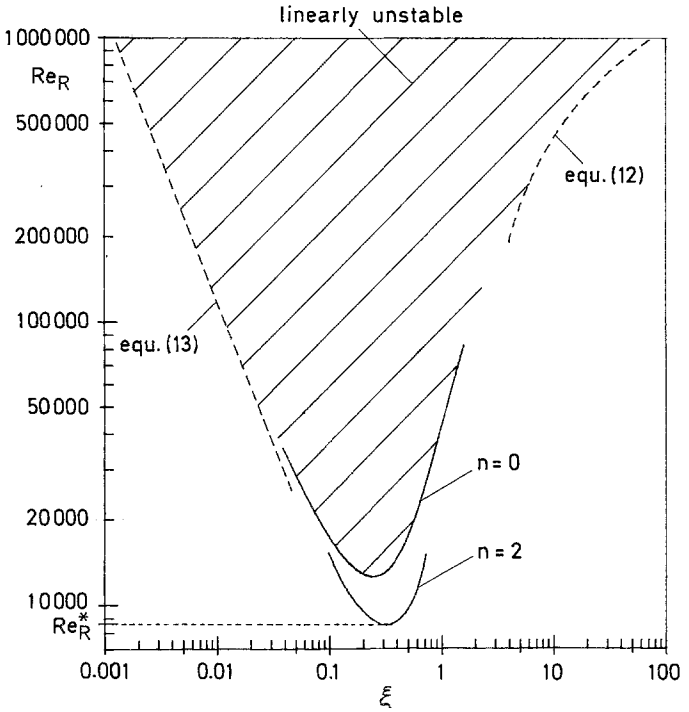

Fig. 10. Stability chart for the axisymmetric laminar boundary layer flow along a semi-infinite cylinder ($n = 2$ from Kao and Chow [6])

It should be noted that this stability boundary does not depend on the displacement thickness of the boundary layer, which is the second length scale entering the problem.

This behaviour is in sharp contrast to the results holding for a classical Blasius boundary layer where the flow destabilizes downstream along the flat plate with decreasing wall shear stress $\tilde{\tau}_W$ if the Reynolds number Re_δ based on the displacement thickness $\tilde{\delta}$ exceeds a critical value $\mathrm{Re}_{\delta_{cr}} = 520$ (cf. Jordinson [5]). Let us consider a hollow cylinder of constant radius $\tilde{R}$ with a sharp leading edge at $\tilde{z} = 0$. For sufficiently large values of Re_R instability sets in in the almost two-dimensional boundary layer near the leading edge and the stability limit of the Blasius flow can be applied. In terms of Re_R and ξ we get the asymptotic expression

$$\mathrm{Re}_{R_{cr}} = 1208.7/\xi \quad \text{for} \quad \xi \to 0 \tag{13}$$

which is shown as a dashed straight line in the double-log diagram, Fig. 10.

Finally, to close the stability chart in the region $\xi = 0(1)$ between the asymptotic results (12) and (13) valid for $\xi \to \infty$ and $\xi \to 0$, respectively, it was necessary to carry out numerical calculations of the full Orr-Sommerfeld problem (4). To each value of ξ belongs a particular velocity profile $W_0(r; \xi)$. These mean flow profiles were determined using the two equation local nonsimilarity method which has been applied to the axisymmetric boundary layer first by Sparrow et al. [13]. Using this velocity distributions $W_0(r; \xi)$ the axisymmetric eigen-value problem (4) yields the neutral-stability curves with the corresponding critical Reynolds numbers $\mathrm{Re}_{R_{cr}}(\xi)$ which are shown in Fig. 10 (curve $n = 0$). These results form the lower boundary of the region of instability and fit very well to the asymptotes (12) and (13).

During the final preparation of this work the author received a copy of a recently published AIAA-paper by Kao and Chow [6]. In their numerical study Kao and Chow considered also non axisymmetric modes for the linear stability problem, characterized by an azimuthal wavenumber

$n \neq 0$. They found that $n = 2$ is the most unstable mode in the boundary layer along the circular cylinder with a minimum Reynolds number $Re_R^* = 8487.5$ at $\xi^* = 0.33$ and their numerical results are depicted in Fig. 10 (curve $n = 2$). The authors just remark that "at a higher value of Re_R the transition value ξ_{tr} shifts to a lower value on the left branch of the critical curve" (Kao and Chow, p. 7 and Fig. 7) but they do not give any comment concerning the "right branch of the critical curve".

According to the present investigation which is restricted to linear theory, pure temporal stability analysis and parallel flow assumption, we can finally characterize the stability behaviour of the boundary layer flow along a circular cylinder as follows. No instability occurs for Reynolds numbers below a critical value Re_R^*. For sufficiently large values $Re_R > Re_R^*$ the flow becomes unstable but inside a confined region downstream the leading edge only. This novel feature of the stabilization of a simple boundary layer flow without pressure gradient is strongly confirmed by the asymptote (12). It would be interesting to study the implications of this behaviour since the logarithmic formula (7) represents the velocity profile on an extremely long cylinder in both laminar and turbulent flow (see White [16]). Further investigations will aim on the influence of non axisymmetric modes on the long wave eigen-value problem [Eq. (5), Fig. 4] and sliding Couette flow (Fig. 8) and on problems of nonlinear perturbations introduced in the boundary layer along the cylinder near the state of "marginal instability" (given by ξ^* and Re_R^*).

References

[1] Cowley, S. J., Smith, F. T.: On the stability of Poiseuille-Couette flow: a bifurcation from infinity. J. Fluid Mech. **156**, 83–100 (1985).

[2] Drazin, P. G., Reid, W. H.: Hydrodynamic stability. Cambridge: Cambridge University Press 1981.

[3] Dzygadlo, Z., Chlebny, B.: Numerical stability analysis of an axially symmetric incompressible viscous flow under three-dimensional perturbations. J. Tech. Phys. Warszawa **24**, 317–338 (1983).

[4] Glauert, M. B., Lighthill, M. J.: The axisymmetric boundary layer on a long thin cylinder. Proc. R. Soc. London Ser. **A 230**, 188–203 (1955).

[5] Jordinson, R.: The flat plate boundary layer, part 1. J. Fluid Mech. **43**, 801–811 (1970).

[6] Kao, K., Chow, C.: Stability analysis of boundary layer on a semi-infinite circular cylinder with and without spin. AIAA-Paper 90-0116 (1990).

[7] Mahadevan, R., Lilley, G. M.: The stability of axial flow between concentric cylinders to asymmetric disturbances. In: Agard Conference Proceedings No. 224, "Laminar-Turbulent Transition", 9/1–9/10 (1977).

[8] Mott, J. E., Joseph, D. D.: Stability of parallel flow between concentric cylinders. Phys. Fluids **11**, 2065–2073 (1968).

[9] Ng, B. S., Reid, W. H.: An initial value method for eigenvalue problems using compound matrices. J. Comput. Physics **30**, 125–136 (1979).

[10] Orszag, S. A.: Accurate solution of the Orr-Sommerfeld stability equation. J. Fluid Mech. **50**, 689–703 (1971).

[11] Potter, M. C.: Stability of plane Couette-Poiseuille flow. J. Fluid Mech **24**, 609–619 (1966).

[12] Preziosi, L., Rosso, F.: Stability of a viscous liquid between sliding pipes. Phys. Fluids **A 2**, 1158–1162 (1990).

[13] Sparrow, E. M., Quack, H., Boerner, C. J.: Local non-similarity boundary layer solutions. AIAA J. **8**, 1936–1942 (1970).

[14] Stewartson, K.: The asymptotic boundary layer on a circular cylinder in axial incompressible flow. Q. Appl. Math. **13**, 113–122 (1955).

[15] Strumolo, G. S.: Perturbed bifurcation theory for Poiseuille annular flow. J. Fluid Mech. **130**, 59–72 (1983).

[16] White, F. M.: Viscous fluid flow. New York: McGraw-Hill 1974.

Author's address: Ph. Gittler, Institute of Fluid Dynamics and Heat Transfer, Technical University Vienna, Wiedner Hauptstrasse 7, A-1040 Vienna, Austria